Frontiers in Heat and Mass Transfer

Tech Science Press

https://doi.org/10.32604/fhmt.2026.078641

ARTICLE

Thermodynamic and Flow Distribution Characteristics of Plate Heat Exchangers with Diversion Grooves Structures

Zeli Wang[1], Bo Zhao[1,2,*], Youliang Chen[1] and Ling Tao[3,*]

[1]Hubei Key Laboratory for Efficient Utilization and Agglomeration of Metallurgic Mineral Resources, Wuhan University of Science and Technology, Wuhan, China

[2]Industrial Safety Engineering Technology Research Center of Hubei Province, Wuhan University of Science and Technology, Wuhan, China

[3]School of Environmental and Biological Engineering, Wuhan Technology and Business University, 3 Huangjiahu West Road, Wuhan, China

*Corresponding Authors: Bo Zhao. Email: zhaobo87@wust.edu.cn; Ling Tao. Email: taoling@wtbu.edu.cn

Received: 05 January 2026; Accepted: 23 March 2026; Published: 29 June 2026

ABSTRACT: Plate heat exchangers are extensively utilized in thermal management. The heat transfer efficiency is significantly constrained by structural parameters and the non-uniformity of flow distribution across the plates. To address this, this study proposes the integration of diversion grooves onto the heat transfer plates to optimize the flow field. Numerical simulations conducted using ANSYS FLUENT demonstrate that the introduction of diversion grooves effectively reduces the fluid distribution uneven coefficient by 6.9%. To identify the optimal configuration, a series of plate models were developed and analyzed, investigating the impact of varying diversion groove lengths (ranging from 0 to 3/4 of the heat transfer zone width), numbers (0, 3, 4, 5, and 6), and corrugated angles (0°, 15°, 30°, 45°, 60°, and 75°). The results indicate that the optimal performance is achieved when the diversion groove length accounts for 2/3 of the main heat transfer zone with a quantity of four grooves. Compared to the baseline structure without diversion grooves, this configuration yields a 26.2% increase in the comprehensive performance coefficient and a 4.6% reduction in the fluid distribution uneven coefficient. Furthermore, under identical diversion groove configurations, the plate with a 60° corrugated angle exhibits superior performance, surpassing other angles by at least 1.4% in the comprehensive performance coefficient, while maintaining the fluid distribution uneven coefficient within 0.5% of the minimum observed value. These findings provide a theoretical basis for the structural optimization of high-efficiency plate heat exchangers.

KEYWORDS: Plate heat exchanger; numerical simulation; flow field distribution; heat transfer performance

1 Introduction

Sustainable development in modern society necessitates the efficient utilization of energy. Increasing the energy efficiency of industrial processes can be achieved by reducing excessive heat loss during the working process. Plate heat exchangers (PHEs) have many characteristics, such as high heat transfer efficiency and wide applicability in various fields. It is commonly used in chemical processing, food manufacturing, shipping, transportation, etc. However, despite their widespread application, the performance of PHEs is frequently compromised by flow maldistribution across the plates. Existing studies indicate that uneven flow distribution not only diminishes the effective heat transfer area but also increases fluid resistance and fouling risks, thereby preventing the equipment from achieving its ideal theoretical performance. Therefore,

optimizing the plate structure to ensure uniform flow distribution is critical for enhancing energy efficiency in industrial applications.

The structural design of PHE is simple, being mainly composed of gaskets for sealing fluids and heat exchange plates [1]. A gasketed plate heat exchanger is one of the most widely used PHEs [2]. The main goal of current research on plate heat exchangers is to improve heat transfer efficiency. The heat transfer enhancement techniques can be classified either as active or passive. Performance improvement can be achieved by optimizing the plate structure [3,4]. Existing studies found that differences in plate structure have a significant impact on heat exchangers. The structure can not only affect the heat transfer efficiency but also influence the flow field distribution [5]. Due to limitations of both physical and chemical methods, some research has changed the flow field between plates by changing the plate structure. Flow field parameters, such as velocity, temperature, and flow rate, all have an impact on heat exchanger performance. The non-uniform flow field can seriously affect the heat transfer efficiency of PHE and increase fluid resistance between plates [6]. Some studies have verified the accuracy of numerical simulation methods for heat transfer processes through software simulation, pointing out that model variations are significantly related to heat transfer performance and energy efficiency [7,8]. Fluid flow velocity is affected by channel size parameters, the increase in flow velocity can lead to an increase in fluid turbulence intensity, which significantly improves heat transfer efficiency [9–11]. Some studies have conducted quantitative experimental research on the effect of uneven flow distribution on heat transfer efficiency, finding that the heat transfer performance of the heat exchanger was decreased by 4% [12]. The change in channel shape has a significant impact on fluid flow. It is considered to affect the performance and resistance of fluids in the heat exchange process by altering the plate conditions [13]. The uneven flow distribution in plate heat exchangers hinders the expected ideal performance. Some studies use the finite element method to simulate flow and optimize the layout of fluid channels in the flow field. They found that changing the structure can improve the flow field distribution, but there is a lack of complete three-dimensional model analysis of the model [14]. In addition, existing studies also found that the uniformity of fluid distribution has a significant impact on flow field characteristics. It is possible to reduce the non-uniform flow field distribution by changing the plate structure [15,16]. The main research on changing plate structure focuses on changing angles, height, and width of the corrugated plate [17–19]. For the influence of different corrugated angles on heat exchangers, compared with plates with a corrugated angle of 35°, the thermal resistance of plates with a corrugated angle of 65° was decreased by 70%, the hot fluid side was increased by 23%, and the pressure drop was increased by 100% [20]. The chevron angle significantly affects the heat transfer rate and turbulence intensity inside the heat exchanger. It demonstrates a positive correlation between the corrugated angle and heat transfer performance, with a substantial enhancement of 35.69% observed in the heat transfer rate as the corrugated angle increases from 30° to 60° [21]. Current research on structural optimization primarily focuses on modifying the corrugated angle, channel height, and depth. However, this improvement comes at a steep cost, higher corrugated angles result in a significant increase in pressure drop. Existing studies have found that as the corrugated angle increases, the Nusselt number of herringbone plates is 2–5 times that of flat plates, while the fluid resistance is 13–44 times higher. At a constant pumping power, the heat transfer of the herringbone a plate is 2.8 times greater than that of flat plate channel [22].

Currently, the structure of heat transfer plates in plate heat exchangers has been extended to a variety of structures, including rectangular, trapezoidal, and triangular configurations [23]. Studies show that different corrugation shapes of corrugations exert a positive optimization effect in improving fluid flow uniformity. To reduce the increase in fluid resistance caused by plate structure optimization, and at the same time improve heat transfer performance, adding flow guide structures to the heat exchange plates is a novel approach. It found that heat transfer performance proved by 20% in helically grooved shell and coil tube heat

exchanger [24], but there is a significant scarcity of literature regarding the application of corrugated grooves in plate heat exchangers. More importantly, existing studies hasn't systematically investigated the coupling effect between diversion groove parameters (length, quantity) and the corrugated angle. It remains unclear whether integrating diversion grooves can effectively mitigate the maldistribution issue in high-angle plates without incurring excessive pressure drops.

To achieve the optimization goal of plate heat exchangers by regulating flow field distribution, this work establishes a complete heat transfer plate model with diversion grooves added to a corrugated plate. This study establishes a complete heat transfer plate model with the addition of deflector grooves to the corrugated plate. Deep insight into the effect of adding grooves on the heat transfer performance of a plate heat exchanger through computational fluid dynamics (CFD) calculation. The study focuses on the effects of the length, number, and corrugated angle of the diversion grooves on the performance of the heat exchanger, and the optimal structural combination is determined through comparison. The findings provide a theoretical basis for the structural optimization of next-generation high efficiency plate heat exchangers.

2 Simulation Methods

2.1 Model Building

This study used "ANSYS FLUENT" computational fluid dynamics software for simulation research. ANSYS is widely used in research on fluid flow and thermodynamics, with the deviation of simulation results falling within an acceptable range, and it is applied to investigate fluid flow conditions in studies of plate heat exchangers [25,26]. Models of heat exchange plates are established based on a certain type of heat exchange equipment in actual, and a three-dimensional model of a heat exchanger plate is established by SolidWorks software, as shown in Fig. 1. It is composed of heat exchange plates and sealing gaskets. Simulations are carried out using different diversion grooves to determine the optimal parameters in terms of thermodynamic and flow distribution. A schematic diagram of the plate structure is shown in Fig. 2. Considering the principle of single variable, the diversion groove is only located on the cold fluid side plate, and the same structure is used for the hot fluid side plate in each model.

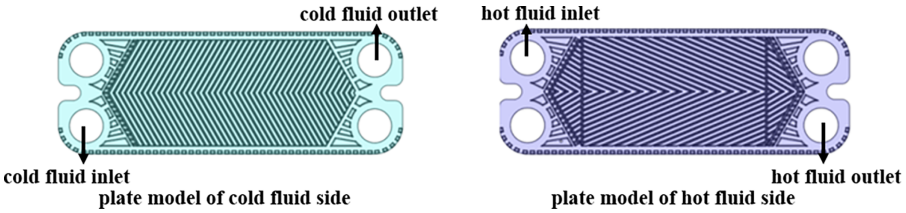

Figure 1: Model of herringbone corrugated heat exchanger plates.

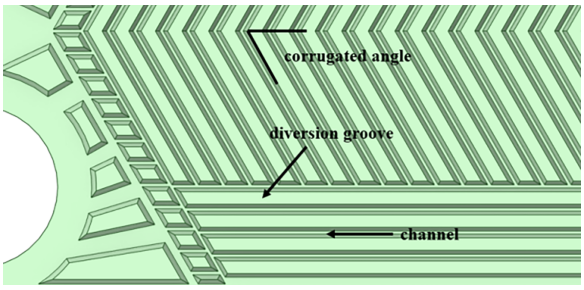

Figure 2: Schematic diagram of plate corrugated angle, diversion groove and channel.

Tetrahedral mesh is suitable for mesh generation of complex curved surfaces or irregular geometric models. In this work, the meshes for the fluid and solid domains employed in the numerical computation consist of tetrahedral elements. Owing to the complex mesh distribution at the flow guide structure, a mesh refinement was applied to the flow guide structure and its vicinity to effectively capture the gradient distributions of temperature and velocity parameters in this region, as shown in Fig. 3.

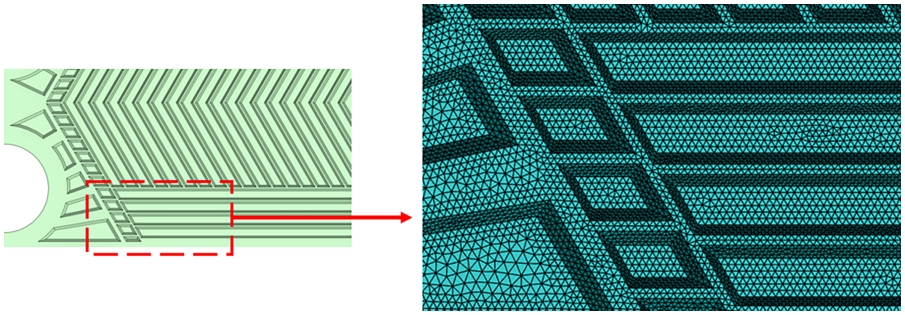

Figure 3: Mesh diagram of the flow guide structure region in the model.

2.2 Boundary Conditions and Governing Equations

Numerical simulations are conducted on two types of plate models, one with added diversion grooves and the other is the original plate, which has no grooves. The effects of adding diversion grooves on the plates are analyzed from the aspects of heat transfer performance and flow field distribution. The boundary conditions are set as follows: cold fluid is liquid water with the inlet temperature of 298 K, and hot fluid is liquid water with the inlet temperature of 373 K. The inlet is set as a velocity inlet, and the outlet is set as a pressure outlet. Planes in the cold and hot fluid domains are selected to study the distribution of the fluid state. After simplification, the fluid flow direction within the plate is as follows: hot fluid enters the plate from a circular hole at the top left corner between plates and exits from a circular hole at the bottom right corner. Cold fluid enters from a circular hole area at the bottom left corner and exits from a circular hole area at the top right corner. This study focuses on the distribution of fluid temperature and velocity.

In ANSYS FLUENT simulations, the coupling relationship between pressure and velocity is the core of solving the Navier-Stokes equations [27]. Fluent provides two primary pressure-velocity coupling solvers: the Coupled algorithm and the SIMPLE algorithm. The Coupled algorithm solves pressure, velocity, as well as temperature, turbulence parameters, as a whole, and is suitable for compressible fluids and strongly coupled problems. In contrast, the SIMPLE algorithm iteratively solves the velocity and pressure fields through pressure correction, making it suitable for low-speed incompressible flows. Compared with the Coupled algorithm, the SIMPLE algorithm offers lower computational cost and better stability. Due to the large number of grids in this study and the high computational requirements, the SIMPLE algorithm is adopted for the heat transfer simulation.

The standard k-ε model needs to solve the equations for turbulent kinetic energy and its dissipation rate. The turbulent kinetic energy transport equation is derived from the exact equation, but the dissipation rate equation is obtained by physical reasoning and mathematical simulation of similar prototype equations. The model assumes that the flow is completely turbulent and that the effect of molecular viscosity is negligible. Therefore, the standard k-ε model is only suitable for the simulation of flow processes with full turbulence. Bai et al. [28] conducted a comparative study of the standard k–ε and realizable k–ε models for plate configurations, demonstrating that the realizable k–ε model with enhanced wall treatment yields higher accuracy in predicting complex turbulent flows within corrugated geometries. Given the findings of this

study and the established suitability of the realizable k-ε model for complex turbulent flows, this model was selected for the subsequent analysis. The steady-state k equation and ε equation are as follows [29]:

$$\rho\overline{u_j}\frac{\partial k}{\partial x_j} = \frac{\partial}{\partial x_j}\left(\frac{\mu_t}{\sigma_k}\frac{\partial k}{\partial x_j}\right) + \mu_t\left(\frac{\partial\overline{u_i}}{\partial x_j} + \frac{\partial\overline{u_j}}{\partial x_i}\right)\frac{\partial\overline{u_i}}{\partial x_j} - \rho\varepsilon \tag{1}$$

$$\rho\overline{u_j}\frac{\partial \varepsilon}{\partial x_j} = \frac{\partial}{\partial x_j}\left(\frac{\mu_t}{\sigma_\varepsilon}\frac{\partial \varepsilon}{\partial x_j}\right) + C_{1\varepsilon}\mu_t\frac{\varepsilon}{k}\left(\frac{\partial\overline{u_i}}{\partial x_j} + \frac{\partial\overline{u_j}}{\partial x_i}\right)\frac{\partial\overline{u_i}}{\partial x_j} - C_{2\varepsilon}\rho\frac{\varepsilon^2}{k} \tag{2}$$

where

$$\mu_t = C_\mu\rho\frac{k^2}{\varepsilon} \tag{3}$$

Mathematical model used for numerical simulation is based on the following assumptions:

1. Heat transfer fluids are all incompressible Newtonian fluids, and the flow regime is steady-state turbulent flow.
2. Gravity and buoyancy due to density differences are neglected because of the low fluid velocity within the heat exchanger.
3. Account only for thermal conduction and thermal convection between the fluid and heat transfer plates, neglecting the influence of thermal radiation.
4. Thermal effect of viscous dissipation during fluid flow is ignored. The model wall is an adiabatic wall, and it is assumed that the system has no heat loss.

A simulation of the heat exchanger follows the laws of mass conservation, momentum conservation and energy conservation. The Navier-Stokes equation describes the conservation of momentum and mass in Newtonian fluids during fluid motion. The N-S equation is the primary governing equation used in ANSYS software to simulate fluid heat transfer. Since the fluid is set to incompressible liquid water, the N-S equation can be simplified as follows:

$$\rho\left(\frac{\partial v_x}{\partial t} + v_x\frac{\partial v_x}{\partial x} + v_y\frac{\partial v_x}{\partial y} + v_z\frac{\partial v_x}{\partial z}\right) = -\frac{\partial p}{\partial x} + \mu\left(\frac{\partial^2 v_x}{\partial x^2} + \frac{\partial^2 v_x}{\partial y^2} + \frac{\partial^2 v_x}{\partial z^2}\right) + \rho g_x \tag{4}$$

$$\rho\left(\frac{\partial v_y}{\partial t} + v_x\frac{\partial v_y}{\partial x} + v_y\frac{\partial v_y}{\partial y} + v_z\frac{\partial v_y}{\partial z}\right) = -\frac{\partial p}{\partial y} + \mu\left(\frac{\partial^2 v_y}{\partial x^2} + \frac{\partial^2 v_y}{\partial y^2} + \frac{\partial^2 v_y}{\partial z^2}\right) + \rho g_y \tag{5}$$

$$\rho\left(\frac{\partial v_z}{\partial t} + v_x\frac{\partial v_z}{\partial x} + v_y\frac{\partial v_z}{\partial y} + v_z\frac{\partial v_z}{\partial z}\right) = -\frac{\partial p}{\partial z} + \mu\left(\frac{\partial^2 v_z}{\partial x^2} + \frac{\partial^2 v_z}{\partial y^2} + \frac{\partial^2 v_z}{\partial z^2}\right) + \rho g_z \tag{6}$$

2.3 Data Processing Methods

Parameters obtained after simulation are processed by the following formula: friction factor (f), total heat transfer coefficient (h_t), fluid distribution uneven coefficient (I_v), comprehensive performance index (η) in the PHE [30–32].

$$f = \frac{2\Delta P\cdot d_e}{L\rho v^2} \tag{7}$$

$$h_t = \frac{1}{\frac{1}{h_1} + \frac{\delta}{\lambda} + \frac{1}{h_2}} \tag{8}$$

$$I_v = \frac{v_{max} - v_{min}}{v_{avg}} \tag{9}$$

$$\eta = \frac{Nu}{f} \tag{10}$$

In the formula, d_e is the characteristic length of channel between plates, h is the convective heat transfer coefficient, λ is the thermal conductivity of water, μ is the dynamic viscosity of water, h_1 and h_2 are the convective heat transfer coefficient at the cold and hot fluid side, δ is the thickness of the plate where heat exchange occurs, v_{max}, v_{min}, v_{avg} represent the maximum velocity, minimum velocity and average velocity of the fluid, respectively. Comprehensive performance index (η) considers the heat transfer performance and flow resistance performance at a time, and fluid distribution uneven coefficient (I_v) reflects the degree of uneven distribution of flow field of different structural plates. The higher I_v of the model, the more uneven the distribution of the flow field. Considering both η and I_v are the main basis for selecting relatively better structural plates.

2.4 Mesh Independence Verification

Considering the complexity of the model's internal structure, the manuscript uses an unstructured tetrahedral mesh to divide the study objects. If the number of meshes is too small, there are not enough meshes to accurately describe the key characteristics of the flow field. Too many meshes accumulate too much discrete equation data and distort the results. The Nusselt number simulated by the model for different mesh numbers is shown in the Table 1.

Table 1: Changes of Nu in plate heat exchanger model with different number of meshes.

Number of Meshes	Nu	Relative Error
1,486,912	81.2	—
3,075,663	84.7	4.3%
6,251,122	87.1	2.8%
10,426,781	88.2	1.3%

The relative error of Nu number corresponding to the number of meshes is analyzed. When the number of meshes increases from 6,251,122 to 10,426,781, the Nu error is less than 2%. Therefore, the manuscript uses about 6,251,122 grids for model division.

3 Result and Discussion

3.1 Diversion Grooves Impact Analysis

To validate the accuracy of the CFD simulation for the plate heat exchanger in this study, a comparison was made between the present study and existing research [33]. In the referenced literature, the corrugation height of the plates was 2 mm, and the gap between heat transfer plates was approximately 0.2 mm, which was similar to the model in the present study. Simulations were performed using the fluid inlet temperature and velocity settings from the referenced literature. The simulated Nu values at Re values of 2500, 3000, and 3500 were 82.5, 93.4, and 102.9, respectively, while the corresponding Nusselt numbers in the reference were approximately 90, 102, and 115, with an average error of approximately 10%. Additionally, with reference to the grid independence verification, the accuracy of the simulation in the present study was validated.

The actual plate model was simulated, and the section in the cold fluid region was selected for fluid flow analysis. Fluid temperature and velocity distribution on the cross-section were shown in Fig. 4, and the cross-section temperature distribution cloud diagram in the upper edge region was shown in Fig. 5.

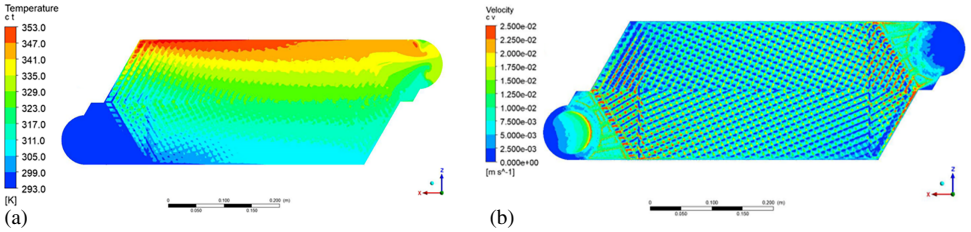

Figure 4: Cloud diagram of temperature and velocity distribution in cold fluid domain: (**a**) Cloud chart of temperature distribution; (**b**) Cloud chart of velocity distribution.

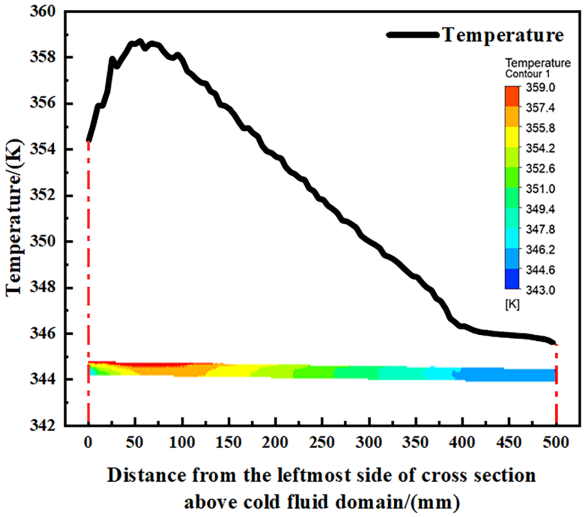

Figure 5: Section temperature distribution above cold fluid domain.

In Figs. 4 and 5, hot fluid of the front and rear plates enters the heat exchange area from the upper left corner, both hot fluid flows in the local area, and the temperatures are high, resulting in a high degree of evaporation of the cold fluid in the upper left corner. When saline fluids are used for heat transfer in actual use, due to the large cold fluid flow in left area, the amount of salt substance precipitating in this area is also large. In order to optimize the flow field distribution, it is considered to make the temperature distribution above the cold fluid more uniform to reduce the average temperature in the upper left corner of the fluid domain. Adding diversion grooves is a useful way to achieve the goal. Fig. 6 presents the velocity vector diagram on the cross-sectional plane of the cold fluid domain. From this figure, it can be observed that the left region exhibits a larger flow rate, and the flow direction of the fluid is influenced by the corrugated structure on the plates. To achieve uniform flow distribution within the fluid domain, adding diversion grooves on the plates is proposed to direct the fluid toward the right region.

3.2 Influence of Diversion Groove Length on Performance and Flow Field of Plate Heat Exchanger

The results from Section 3.1 show that there are more cold fluids in left area, and there is an uneven distribution of the flow field in the fluid channel between plates. It is considered to divert cold fluid to the right by adding a diversion groove to reduce the flow of cold fluid flow in left area to improve the flow field distribution. The model changes are shown in Fig. 7.

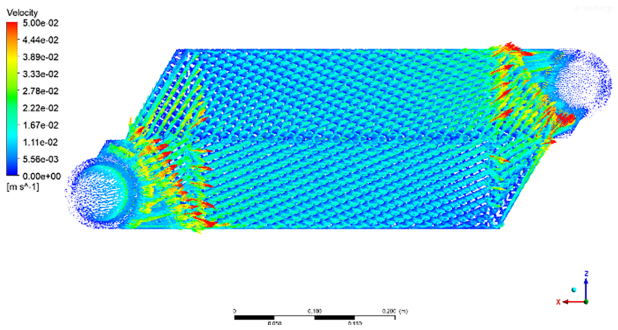

Figure 6: Cross sectional velocity vector diagram of cold fluid domain.

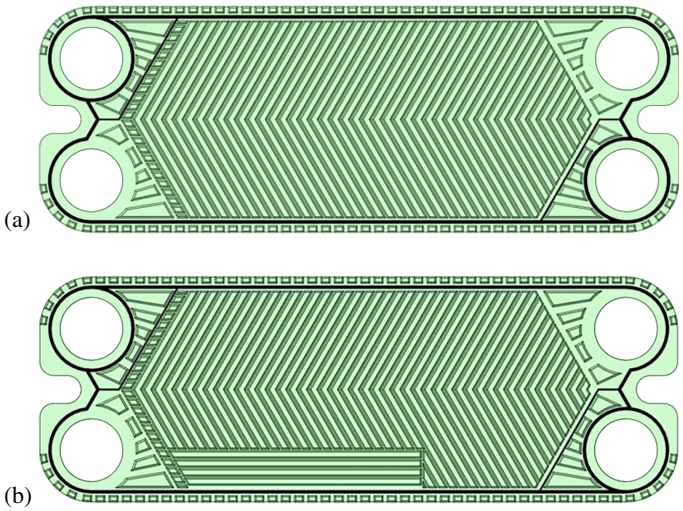

Figure 7: Traditional model at cold fluid side and model with diversion grooves: (**a**) Traditional model of cold fluid side plate without diversion groove; (**b**) Model of cold fluid side plate added into diversion grooves.

After adding diversion grooves, the influence of diversion groove length and numbers on the heat exchanger is mainly studied. Corrugated area in the middle of the plate is the main heat exchange area of the PHE. Six models with the length of the diversion groove as 0, 1/4, 1/3, 1/2, 2/3, and 3/4 of the cross-section in the main heat exchange zone are designed for simulation. Temperature and velocity distribution on the cold fluid side and the hot fluid side are shown in Figs. 8 and 9.

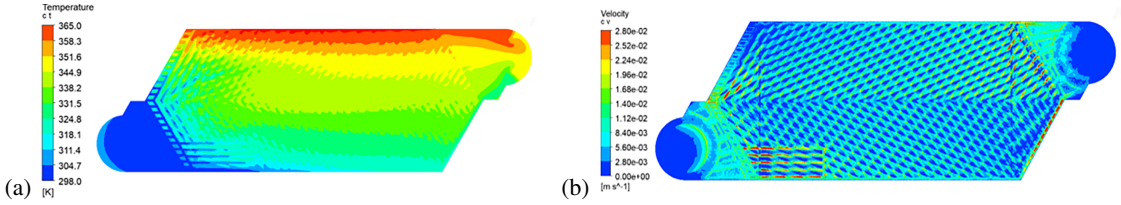

Figure 8: Cloud chart of plane temperature and velocity distribution in cold fluid domain: (**a**) Cloud chart of temperature distribution; (**b**) Cloud chart of velocity distribution.

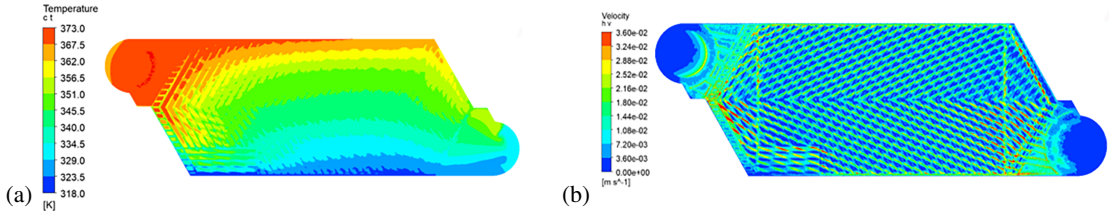

Figure 9: Cloud chart of plane temperature and velocity distribution in hot fluid domain: (**a**) Cloud chart of temperature distribution; (**b**) Cloud chart of velocity distribution.

Compared with the simulation results before and after optimization, cold fluid moved to the right after adding a diversion groove, the average temperature in the area far from cold fluid inlet decreased, mass flow rate in right side of the cold fluid domain increased, the mass flow rate of cold fluid in left area decreased, which improved flow field distribution in the cold fluid. Therefore, plates designed with diversion grooves are more suitable compared with the original plate structure. In order to visually compare the simulation results of different structures, a plate model with the length of diversion groove set to 0 of the section length of the main heat exchange zone is selected as the control model. The normalized comparison method is adopted; the parameter of the control plate is selected as 1.

In Fig. 10a, it can be seen that the heat transfer coefficient in the cold and hot fluid domains first increases and then decreases as the length of the diversion groove increasing. In Fig. 10b, on the basis of keeping the hot fluid side plate unchanged, the friction factor of the hot fluid increases slowly with the increase of diversion groove length, and the friction factor of the cold fluid increases first and then decreases due to the drainage effect of diversion groove. In Fig. 10c, considering the heat transfer performance and resistance characteristics of the plate, when the length of the diversion groove accounts for 2/3 and 3/4, the comprehensive performance index of the plate is higher. The fluid distribution uneven coefficient reaches its maximum value at 1/4 length, increasing by 3.5% compared to the control model. Reaching the minimum value at 1/2 length, it decreased by 6.9% compared to the control model. The uneven flow distribution on the left and right sides of the original plate is quite severe. The medium length diversion groove can directly introduce the fluid from the left side into the middle area to achieve a better flow field distribution balance.

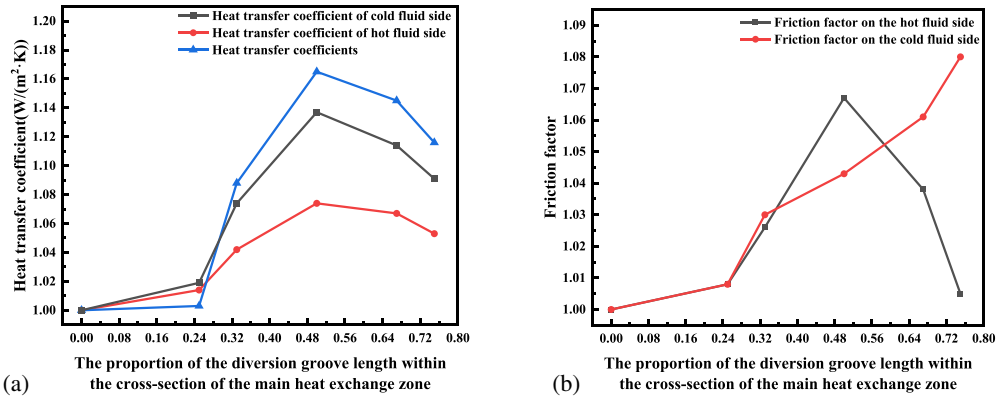

Figure 10: (Continued)

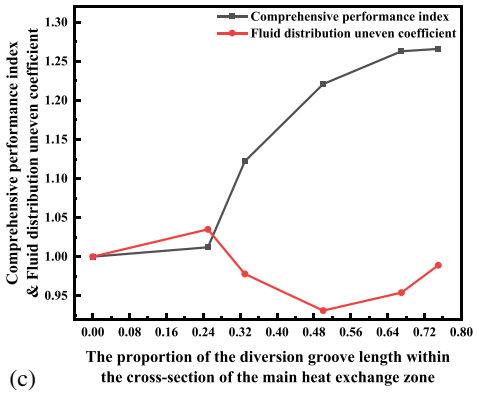

Figure 10: Key parameters of plates with different diversion groove lengths: (**a**) Comparison of heat transfer coefficients of plates; (**b**) Comparison diagram of friction factors of plates; (**c**) Comparison diagram of comprehensive performance index and fluid distribution uneven coefficient of plates.

Table 2 shows the performance of plates with different diversion groove lengths; the model of length 0 has no diversion groove. Upon comparing models with different structures, it was found that the diversion groove significantly affects the performance of the heat exchanger. The results indicate that plates with relatively better comprehensive performance index at the cold end are those with the diversion groove lengths accounting for 2/3 and 3/4, and that plates with relatively better fluid distribution uneven coefficient are those with diversion groove lengths accounting for 1/2 and 2/3. When the length ratio of diversion groove increases from 1/2 to 2/3, compared to the model without a diversion groove, yhe comprehensive performance index of the cold side increases by 22.1% and 26.3%, but the fluid distribution uneven coefficient decreases by 6.9% and 4.6%. When the proportion of the length of the diversion groove increases from 2/3 to 3/4, the comprehensive performance index increases by 26.3% and 26.6%, but the fluid distribution uneven coefficient changed from a decrease of 4.6% to an increase of 1.1%. The diversion groove hinders the upward and downward movement of the fluid. Some of the cold fluid moves to the right along the channel between the diversion grooves, and a small part of the cold fluid jumps out of the diversion groove. The cross arrangement of diversion groove outlet and the corrugation prevents the fluid from entering the corrugation heat transfer zone, which increases the degree of fluid turbulence, then increases heat transfer capacity and resistance characteristics. However, when the diversion groove is too long, fluid moves to the right side along the guide channel.

Table 2: Performance table of plates with different diversion groove lengths (compared with the plate model without diversion groove).

Proportion of Diversion Groove Length in Cross Section Length of Heat Exchange Zone	0	1/4	1/3	1/2	2/3	3/4
Heat transfer coefficient of cold fluid side ($W/m^2 \cdot K$)	1	1.019	1.074	1.137	1.114	1.091
Heat transfer coefficient of hot fluid side ($W/m^2 \cdot K$)	1	1.014	1.042	1.074	1.067	1.053
Heat transfer coefficients ($W/m^2 \cdot K$)	1	1.003	1.088	1.165	1.145	1.116
Cold fluid side friction factor	1	1.008	1.026	1.067	1.038	1.005
Hot fluid side friction factor	1	1.008	1.030	1.043	1.061	1.080
Fluid distribution uneven coefficient	1	1.035	0.978	0.931	0.954	0.989
Comprehensive performance index of cold side	1	1.012	1.122	1.221	1.263	1.266

The reduction of the heat transfer area leads to the decline of heat transfer capacity and resistance characteristics. The heat transfer coefficient and cold fluid friction factor show a trend of first increasing and then decreasing. When a plate model with the length of diversion groove is 1/2 of the section length of the main heat exchange zone, both the heat transfer coefficient and cold fluid friction factor reach their maximum. The heat transfer coefficient is increased by 16.5%, and the cold fluid friction factor is increased by 13.7% compared with the control model coefficient. By processing data and considering the thermodynamic performance and flow field distribution, the effect of plates with a length ratio of 2/3 performs the best among plates with different diversion groove lengths.

3.3 Influence of Diversion Groove Number on Performance and Flow Field of Plate Heat Exchanger

On the basis that the length of the diversion groove is 2/3 of the cross-section length in the main heat exchange zone and the corrugated angle of the plate is 60°, five kinds of plate structures with 0, 3, 4, 5, and 6 diversion grooves on the cold fluid side plate are designed for simulation. A plate model with 0 diversion grooves is selected as the control model. The normalized comparison method is adopted, and the parameter of the control plate is selected as 1.

In Fig. 11a, with the increase of the number of diversion grooves, the heat transfer coefficient in the cold and hot fluids show a continuous growth trend. When the number of diversion grooves is six, the heat exchange effect between fluids is optimal. In Fig. 11b, the fluid friction factor increases with the increase in the number of diversion grooves. In Fig. 11c, through the calculation of the comprehensive performance index, the combined effect of the heat transfer performance and resistance characteristics of plates is analyzed. When the number of diversion grooves is four, the comprehensive performance of the plates is the best, but the fluid distribution uneven coefficient is not optimal. Due to the interference of diversion grooves on fluid flow, the fluid distribution uneven coefficient shows an upward trend with the increase in the number of diversion grooves.

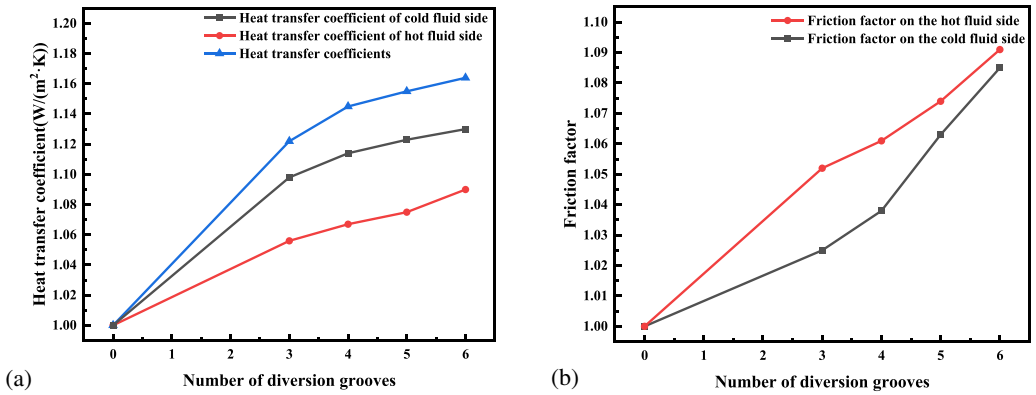

Figure 11: (Continued)

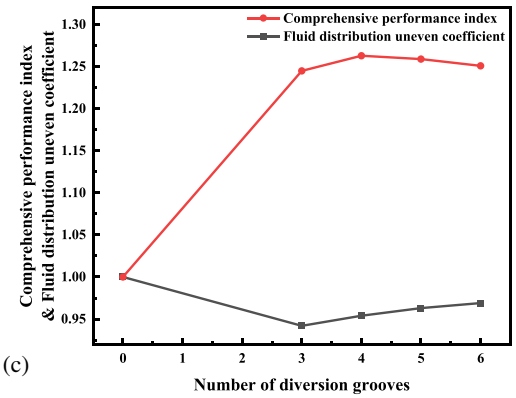

Figure 11: Key parameters of plates with different diversion groove number: (**a**) Comparison of heat transfer coefficients of plates; (**b**) Comparison diagram of friction factors of plates; (**c**) Comparison diagram of comprehensive performance index and fluid distribution uneven coefficient of plates.

Table 3 presents the performance of plates with different numbers of diversion grooves, indicating that plates with four and five diversion grooves have relatively better overall cold fluid side performance index, while plates with three diversion grooves exhibits a relatively better the fluid distribution uneven coefficient. Compared to the plate without diversion grooves, when the number of diversion grooves increases from four to five, the overall cold fluid side performance index increases by 26.3% and 25.9%, and the fluid distribution uneven coefficient reduces by 4.6% and 3.7%. Through data processing, it can be concluded that the number of diversion grooves has little effect on the thermodynamic performance and flow field distribution of the PHE.

Table 3: Performance of plates with different number of diversion grooves (compared with the plate model without diversion groove).

Number of Diversion Grooves	0	3	4	5	6
Heat transfer coefficient of cold fluid side ($W/m^2 \cdot K$)	1	1.098	1.114	1.123	1.130
Heat transfer coefficient of hot fluid side ($W/m^2 \cdot K$)	1	1.056	1.067	1.075	1.090
Heat transfer coefficients ($W/m^2 \cdot K$)	1	1.122	1.145	1.155	1.164
Cold fluid side friction factor	1	1.025	1.038	1.063	1.085
Hot fluid side friction factor	1	1.052	1.061	1.074	1.091
Fluid distribution uneven coefficient	1	0.942	0.954	0.963	0.969
Comprehensive performance index of cold side	1	1.245	1.263	1.259	1.251

In Fig. 12, fluid flow is obviously restrained by the plate corrugation when the fluid flows out of the diversion groove and enters the corrugated heat exchange zone. The interference effect of the heat exchange plate on fluid flow increases with the increase in the number of corrugations. The heat transfer effect and the resistance characteristics of the fluid increase.

In Fig. 13, the fluid motion trajectories near the diversion groove are magnified and displayed to investigate the reasons why this structure affects the performance of the heat exchanger. The trajectories near the diversion groove are dense and uniformly distributed, indicating full utilization of the heat transfer area in the heat exchange region. The trajectories closely adhere to the walls of the guide structure, exhibiting periodic fluctuations. Due to the inclination angle between the fluid flow direction and the guide structure

as well as the V-shaped corrugations, the trajectories display the V-shaped pattern, which subsequently generating a three-dimensional spiral flow. These phenomena enhance the turbulence intensity of the fluid, thereby improving the heat transfer performance.

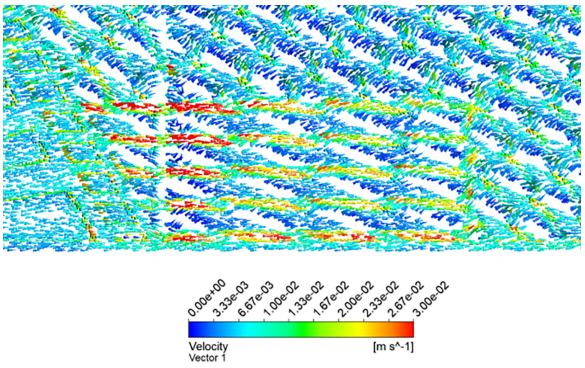

Figure 12: Local flow field in cold fluid domain.

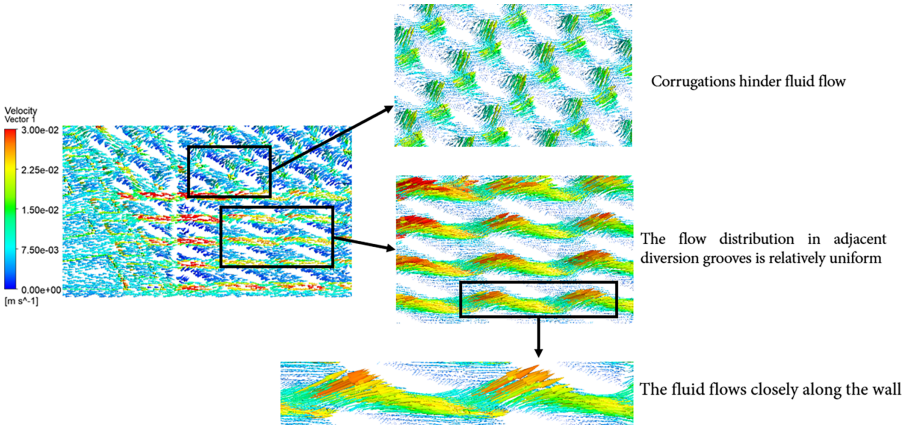

Figure 13: Magnified view of fluid motion trajectories in the local region of the flow guide structure.

In traditional V-shaped plates, the fluid motion opposes the corrugations, which increases the resistance experienced by the fluid while achieving sufficient heat transfer. In contrast, the presence of the diversion groove alleviates the impact of some fluid on the corrugations, resulting in a relatively uniform flow distribution between channels and a relatively balanced pressure drop during fluid flow and heat transfer.

It can be found that the change of the number of corrugations has a greater impact on the local area, but has a smaller impact on the overall performance. In these models with different numbers of diversion grooves, the comprehensive performance index and fluid distribution uneven coefficient corresponding to different numbers of corrugations have changed by 1.8% and 2.7%. The plate model with the three channels and four diversion grooves has the optimal performance.

3.4 Influence of Plate Corrugated Angle on the Performance and Flow Field of Plate Heat Exchanger after Adding Diversion Groove

From the above results, the length of the diversion groove is 2/3 of the cross-section length in the main heat exchange zone, and the effect of performance is relatively optimal when the number of diversion grooves is 4. On the basis of the remaining parameters unchanged, six kinds of plate structures with corrugated angles

of 0°, 15°, 30°, 45°, 60°, and 75° on the cold fluid side plate are selected for simulation. In order to visually compare simulation results of different structures, a plate model with a corrugated angle of 0 in the cold fluid side plate is selected as the control model. The normalized comparison method is adopted, and the parameter of the control plate is selected as 1.

In Fig. 14a, with the increase of corrugated angles, the heat transfer coefficient increases gradually, and the fluid friction factor rises sharply. Referring to the research and analysis without the diversion grooves, with the increase in the corrugated angle, the fluid flow between plates gradually changes from two-dimensional flow to cross flow, and the increase in the contact between fluid and plate makes the fluid flow more disordered [34]. In Fig. 14b, the resistance of fluid between the plates increases due to the increase of the interference of diversion grooves and the corrugated on the fluid. In Fig. 14c, the fluid distribution uneven coefficient shows a gradual decrease trend, but the comprehensive performance index shows a trend of firstly increasing and then decreasing. The comprehensive performance index is increased by 26.2% compared with the control model coefficient.

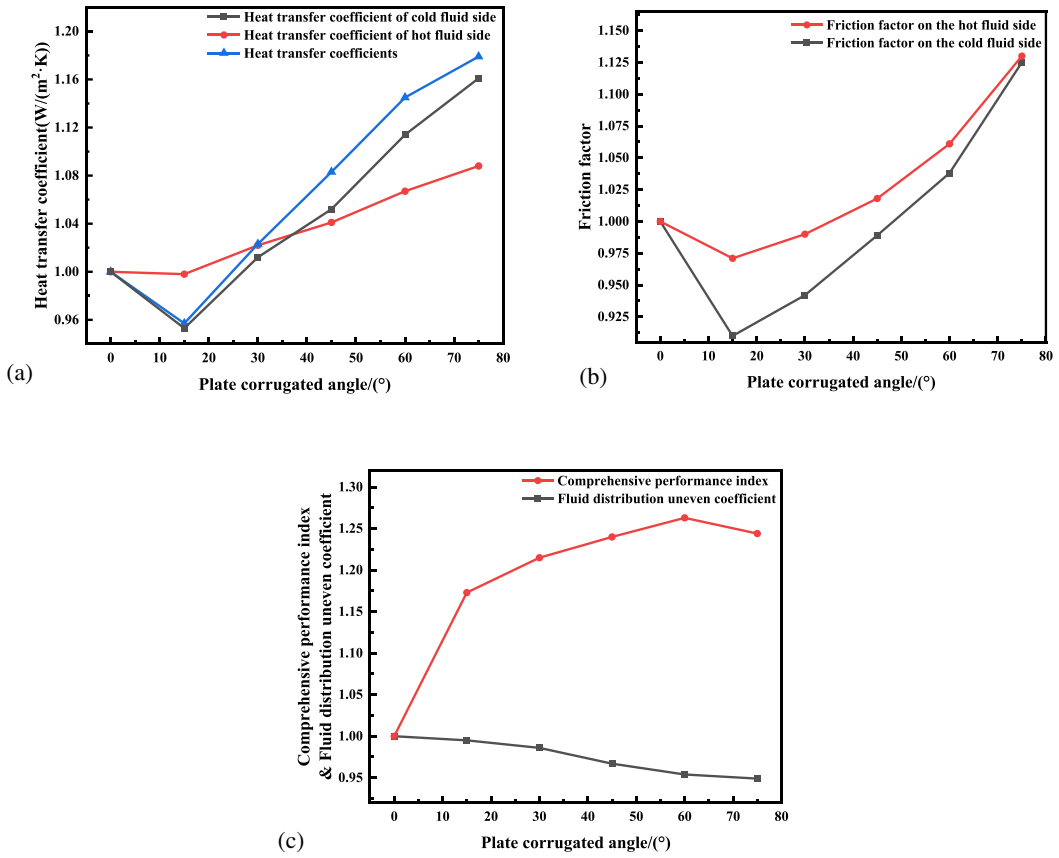

Figure 14: Key parameters of plates with different corrugated angle: (**a**) Comparison of heat transfer coefficients of plates; (**b**) Comparison diagram of friction factors of plates; (**c**) Comparison diagram of comprehensive performance index and fluid distribution uneven coefficient of plates.

Table 4 shows the performance of the plates with different corrugated angles after adding diversion grooves. PHE design typically requires high heat transfer performance, from the perspective of the comprehensive performance index on the cold fluid side, plates with 60° and 75° corrugated angles exhibit relatively superior results. The comprehensive performance index increases first and then decreases with the increase in corrugated angle. The index is the highest when the corrugated angle is 60°, which is 26.2% higher than

the value at the worst angle of 0. Meanwhile, the uniformity of the flow field distribution increases with the increase in the corrugated angles. Therefore, the primary analysis focuses on the performance of plates with corrugated angles of 60° and 75°. Compared with the plate with a corrugated angle of 0, when the corrugated angle increases from 60° to 75°, the fluid distribution uneven coefficient decreases by only 0.5%, whereas the comprehensive performance index drops significantly by 1.8%. The effect of corrugated angles on the flow field is mainly to change the tangential force component, and the flow direction angle of fluid in channel direction also changes, resulting in a change in the turbulence degree of the heat exchange fluid between plates [35]. Change of the flow state not only improves the turbulence degree of the cold fluid flow, but also increases the resistance of fluids. By processing the data and considering the thermodynamic performance and flow field distribution, a corrugated angle of 60° is the best angle among the above corrugated angles model with the addition of a diversion groove.

Table 4: Performance of plates with different corrugated angles (comparison with the plate model with corrugated angle of 0).

Corrugated Angles	0°	15°	30°	45°	60°	75°
Heat transfer coefficient of cold fluid side ($W/m^2 \cdot K$)	1	0.953	1.012	1.052	1.114	1.161
Heat transfer coefficient of hot fluid side ($W/m^2 \cdot K$)	1	0.998	1.022	1.041	1.067	1.088
Heat transfer coefficients ($W/m^2 \cdot K$)	1	0.957	1.023	1.083	1.145	1.179
Cold fluid side friction factor	1	0.910	0.942	0.989	1.038	1.125
Hot fluid side friction factor	1	0.971	0.990	1.018	1.061	1.130
Fluid distribution uneven coefficient	1	0.995	0.986	0.967	0.954	0.949
Comprehensive performance index of cold side	1	1.173	1.215	1.240	1.262	1.244

3.5 Comparative Analysis with Literature

Previous studies have involved optimizing the structure of heat exchanger plates to improve heat transfer performance. A comparison of their key parameters with those in this study is shown in Table 5.

In existing studies, the optimization of heat exchanger plates is primarily categorized into two types: variations in corrugation angles in V-shaped plates, and the remaining corrugation structures not limited to V-shaped plates. Khan et al. limited their study to a corrugation angle of 30° to 60° and did not optimize the corrugation structure. Meanwhile, existing literature mainly focuses on optimizing the corrugation angle between 30° and 60° [37,38]. Lee and Lee [39] expanded the range of corrugation angles to investigate their heat transfer performance and fluid flow resistance. The present study combines these two aspects via η to quantify the comprehensive performance. Kim and Park [40] also consider the results of Nu and f simultaneously, but this study further investigates the optimization of non-uniform coefficients. Some studies [41,42] have caused an increase in fluid resistance and a decline in overall performance by modifying V-shaped plates.

Through comparative analysis, it is evident that the guide groove structure exhibits heat transfer performance similar to or even better than that of other optimized plate models. Moreover, the design of the guide groove structure in this study accounts for optimizing non-uniform fluid flow, thereby endowing it with certain advantages among the various optimized plate models aimed at enhancing heat exchanger performance.

Table 5: Comparison of key parameters between this study and existing studies.

Authors	Structural Optimization	Key Findings
Khan et al. [36]	Corrugation angle	Nu increases by approximately 2.8 times when the corrugation angle is changed from 30° to 60°.
Krishna et al. [37]	Corrugation angle	When the corrugation angle is increased by 30°–40°, the Nu increases by 15%. When the corrugation angle is increased by 40°–50°, Nu increases by 30%.
Hessami [38]	Corrugation angle	As corrugation angle changes from 45° to 60°, Nu and f increase by 1.5–2 times.
Lee and Lee [39]	Corrugation angle	Friction factor increases by about 109% and 273%, as β increases from 30° to 60°.
Kim and Park [40]	Plates with different chevron shapes and hydraulic diameters	Thermal and hydraulic performance exhibits a slight improvement as the $j/f^{1/3}$ value increases from 1.17 to 1.22.
Kim et al. [41]	Double-wave plate	Heat transfer performance and ΔP of a double-wave PHE increase by 50% and 30%, respectively, compared with a chevron corrugation PHE.
Luan et al. [42]	Transverse and longitudinal corrugation	Anti-phase secondary corrugation exhibits the best performance. Compared with chevron corrugation PHEs, the Nu and f of compound corrugation PHE decrease by 25% and 50%, respectively.
This study	Guide groove structure	After adding the guide groove structure, the total heat transfer coefficient and comprehensive performance coefficient of the PHE increased by 14.5% and 26.2%, respectively. And the fluid distribution uneven coefficient decreased by 4.6%.

3.6 Mechanical Study of Plate Structure

A stress-strain curve depicts the relationship between a material's stress and strain under external forces, while also indicating its mechanical properties and deformation behavior. Typically, metallic materials exhibit elastic deformability. When loaded beyond its yield strength, the material experiences plastic deformation until failure. This process is represented in the stress-strain curve by four stages: elastic, yield, strengthening, and local deformation.

In Fig. 15, the model simulates stress values by applying different strain conditions under varying flow velocities, with the stress-strain curves for the three flow velocity models presented. The results show that the simulation primarily focuses on the elastic stage. During the elastic stage, the cessation of heat transfer results in stress relief and subsequent deformation recovery. In this state, the mechanical impact of the heat transfer process on the plate is recoverable, resulting in minimal damage. Fig. 15 indicates that with the addition of the guide groove structure, the plate's mechanical strength remains within an acceptable range.

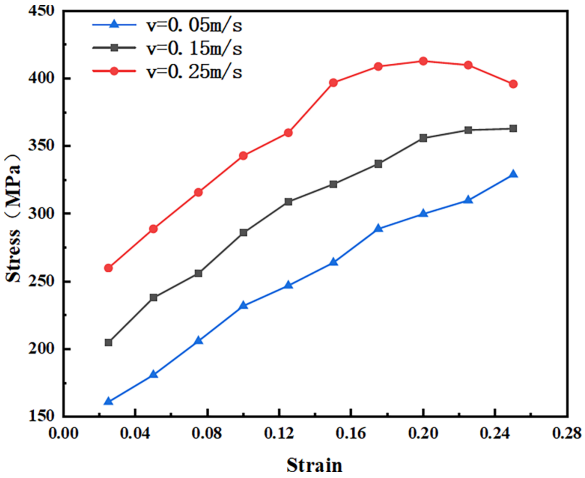

Figure 15: Stress-strain curves of models with different flow velocities.

4 Conclusion

Through simulations of various heat transfer plate structures, it is observed that the uneven distribution in the fluid channel is obvious in some areas. By changing part of the plate corrugated angles into the drainage groove structure, the cold fluid is introduced into the area with lower flow rates, which will result in alleviating the uneven distribution of the flow field is alleviated. When the length of the diversion groove is 2/3 of the cross-section in the main heat exchange zone, and the number of diversion grooves is 4, which have 3 diversion channels, thermodynamic performance and the effect of flow field distribution of the diversion grooves are the best. The corrugated angle of the cold fluid side plate is changed on the basis of the best diversion groove matching scheme.

The comprehensive performance index of the plate with a 60° corrugated angle is improved by 26.2% compared to the plate without a corrugated angle, and the fluid distribution uneven coefficient is decreased by 4.6%. When PHEs with diversion grooves at different corrugated angles are compared, considering both heat transfer performance and flow field distribution, the plate with a 60° corrugated angle has the best overall performance. This study focuses on the diversion groove structure and finds that it has a positive effect on the heat transfer performance and fluid flow distribution of plate heat exchangers. In existing literature, enhancing heat transfer performance by modifying heat transfer plate structures often leads to a significant increase in fluid resistance. In contrast, the presence of the guide groove structure prevents fluid accumulation, guides fluid flow, effectively alleviates non-uniform distribution during the heat transfer process, and on this basis, achieves improved heat transfer performance of plate heat exchangers.

The findings of this study provide new insights for research focusing on surface structure optimization of heat transfer plates, and lay a solid foundation for future research for the further exploration of the impact of heat transfer plates incorporating diversion groove structures on heat exchanger performance during heat transfer processes with fluids of different physical properties.

Acknowledgement: Not applicable.

Funding Statement: This work was supported by the Natural Science Foundation of Wuhan (2025041001010356), Hubei Provincial Department of Education Science and Technology Plan Project (B2018308), Hubei Provincial Teaching Reform Research Project for Graduate Education (2025670).

Author Contributions: Research design concept: Bo Zhao, Ling Tao, Zeli Wang; model building and simulation: Youliang Chen, Zeli Wang; analysis and interpretation of results: Ling Tao, Bo Zhao; draft manuscript preparation: Zeli Wang, Bo Zhao. All authors reviewed and approved the final version of the manuscript.

Availability of Data and Materials: The data are available from the corresponding authors upon reasonable request.

Ethics Approval: The article does not include human participants and/or animals research.

Conflicts of Interest: The authors declare no conflicts of interest.

Nomenclature

$C_{1\varepsilon}$, $C_{2\varepsilon}$, C_{μ}	Turbulence model coefficient
f	Friction factor
h	Convective heat transfer coefficient
I_v	Fluid distribution uneven coefficient
k	Turbulent kinetic energy J/kg
L	Channel length mm
Nu	Nusselt number
Pr	Prandtl Number
Re	Reynolds number
v	Fluid velocity m/s
ΔP	Pressure drop Pa
β	Corrugated angle °
δ	Plate thickness mm
η	Comprehensive performance index
ε	Turbulent kinetic dissipation J/kg·s
λ	Coefficient of thermal conductivity W/m·K
μ	Dynamic viscosity Pa·s
ρ	Density kg/m^3
σ_k, σ_ε	Turbulent coefficient
h_t	Heat transfer coefficients W/m^2·K
d_e	Interplate channel characteristic length mm

References

1. Arima H, Nishiguchi M, Suehiro S. Effect of the surface form of the herringbone aluminum plate in a plate heat exchanger on the boiling heat transfer performance of ammonia. Appl Therm Eng. 2024;256(2):124057. doi:10.1016/j.applthermaleng.2024.124057.
2. Zhang J, Zhu X, Mondejar ME, Haglind F. A review of heat transfer enhancement techniques in plate heat exchangers. Renew Sustain Energy Rev. 2019;101:305–28. doi:10.1016/j.rser.2018.11.017.
3. Bergles AE. The implications and challenges of enhanced heat transfer for the chemical process industries. Chem Eng Res Des. 2001;79(4):437–44. doi:10.1205/026387601750282562.
4. Nahes ALM, Costa ALH, Bagajewicz MJ. A new approach for the globally optimal design of gasketed plate heat exchangers with variable properties. Chem Eng Sci. 2023;280(4):119067. doi:10.1016/j.ces.2023.119067.
5. Hassanzadeh R, Abadtalab M, Bayat A. Optimization of wave inclination angle in parallel wavy-channel heat exchangers. Arab J Sci Eng. 2020;45(2):817–32. doi:10.1007/s13369-019-04145-6.
6. Yoon W, Jeong JH. Development of a numerical analysis model using a flow network for a plate heat exchanger with consideration of the flow distribution. Int J Heat Mass Transf. 2017;112(4):1–17. doi:10.1016/j.ijheatmasstransfer.2017.04.087.

7. Liu Y, Jia T, Wang J, Li Y, Zhao J, Wang Y, et al. Research on the energy efficiency improvement of closed loop wastewater source heat pump with direct-expansion heat exchanger. Therm Sci. 2024;28(5 Part B):4067–80. doi:10.2298/tsci231223115l.
8. Wang T, Ma S. Thermoelectric generator heat performance study about improved fin structures. Therm Sci. 2018;22(1 Part A):101–12. doi:10.2298/tsci150801064w.
9. Srihari N, Das SK. Experimental and theoretical analysis of transient response of plate heat exchangers in presence of nonuniform flow distribution. J Heat Transf. 2008;130(5):051801. doi:10.1115/1.2885153.
10. Srihari N, Prabhakara Rao B, Sunden B, Das SK. Transient response of plate heat exchangers considering effect of flow maldistribution. Int J Heat Mass Transf. 2005;48(15):3231–43. doi:10.1016/j.ijheatmasstransfer.2005.02.032.
11. Eldeeb R, Aute V, Radermacher R. Pillow plate heat exchanger weld shape optimization using approximation and parallel parameterized CFD and non-uniform rational B-splines. Int J Refrig. 2020;110(5):121–31. doi:10.1016/j.ijrefrig.2019.10.024.
12. Beckedorff L, da Silva RPP, Martins GSM, de Paiva KV, Oliveira JLG, Oliveira AAM. Flow maldistribution and heat transfer characteristics in plate and shell heat exchangers. Int J Heat Mass Transf. 2022;195(8):123182. doi:10.1016/j.ijheatmasstransfer.2022.123182.
13. Nashee S, Mushatet K. Performance study on turbulent heat transfer using rectangular air duct integrated with continuous and intermittent ribs turbulators. Therm Sci. 2025;29(2 Part A):955–67. doi:10.2298/tsci240430214n.
14. Gersborg-Hansen A, Sigmund O, Haber RB. Topology optimization of channel flow problems. Struct Multidiscip Optim. 2005;30(3):181–92. doi:10.1007/s00158-004-0508-7.
15. dos Santos FJ, Silva RPP, de Paiva KV, Oliveira JLG. Evaluation of plate heat exchangers comprising sections with different chevron angle arrangements. Appl Therm Eng. 2024;249(4):123452. doi:10.1016/j.applthermaleng.2024.123452.
16. Burgers JG, Lemczyk TF. Optimization of louvered fins in intermittent contact with plate heat exchanger passageways. SAE Tech Pap Ser. 1988;1:880447. doi:10.4271/880447.
17. Nithya M, Senthil Vel M, Anitha S, Sivaraj C. Optimizing thermal efficiency: advancements in flat plate heat exchanger performance through baffle integration. Int Commun Heat Mass Transf. 2024;158(22):107885. doi:10.1016/j.icheatmasstransfer.2024.107885.
18. Kapustenko P, Klemeš JJ, Arsenyeva O. Plate heat exchangers fouling mitigation effects in heating of water solutions: a review. Renew Sustain Energy Rev. 2023;179(1):113283. doi:10.1016/j.rser.2023.113283.
19. Abeywickrama J, Grimmer M, Hoth N, Grab T, Drebenstedt C. Geochemical characterization of fouling on mine water driven plate heat exchangers in Saxon mining region. Germany Int J Heat Mass Transf. 2021;176:121486. doi:10.1016/j.ijheatmasstransfer.2021.121486.
20. Arsenyeva O, Matsegora O, Kapustenko P, Yuzbashyan A, Jaromír Klemeš J. The water fouling development in plate heat exchangers with plates of different corrugations geometry. Therm Sci Eng Prog. 2022;32:101310. doi:10.1016/j.tsep.2022.101310.
21. Methekar N, Kotian S, Jain N, Vartak P, Naik P, Nikam S, et al. Numerical investigation of thermohydraulic characteristics of a gasketed plate heat exchanger. Comput Thermal Scien. 2022;14(1):61–102. doi:10.1615/computthermalscien.2021039019.
22. Sohn S, Shin JH, Kim J, Yoon SH, Lee KH. A numerical study on the pressure drop and heat transfer in the hot channel of plate heat exchanger with chevron shape. Korean J Air Cond Refrig Eng. 2018;30(4):175–85. doi:10.6110/kjacr.2018.30.4.175.
23. Soomro KA, Rai R, Qureshi SR, Kumarasamy S, Memon AH, Jamil R. CFD analysis of corrugated plate designs to improve heat transfer efficiency in plate heat exchangers. Energy Eng. 2025;122(12):4857–72. doi:10.32604/ee.2025.069847.
24. Miansari M, Darvishi MR, Toghraie D, Barnoon P, Shirzad M, Alizadeh A. Numerical investigation of grooves effects on the thermal performance of helically grooved shell and coil tube heat exchanger. Chin J Chem Eng. 2022;44(22):424–34. doi:10.1016/j.cjche.2021.05.038.

25. Frota MN, Ibañez Aguillar IF, De La Hoz Truyoll SL. Leveraging CFD simulation to optimize the flow of cleaning artifacts to remove scale from heat transfer surfaces of heat exchangers. Meas Sens. 2025;38(15–16):101574. doi:10.1016/j.measen.2024.101574.
26. Niezgoda-Żelasko B, Kuchmacz J. CFD modelling of the flow of ice slurry in plate heat exchanger channels. Energy. 2025;317(1):134700. doi:10.1016/j.energy.2025.134700.
27. Wang W, Zhang Y, Li Y, Han H, Li B. Numerical study on fully-developed turbulent flow and heat transfer in inward corrugated tubes with double-objective optimization. Int J Heat Mass Transf. 2018;120:782–92. doi:10.1016/j.ijheatmasstransfer.2017.12.079.
28. Bai C, Zhang G, Qiu Y, Leng X, Tian M. A new method for heat transfer and fluid flow performance simulation of plate heat exchangers. Numer Heat Transf Part B Fundam. 2019;75(2):93–110. doi:10.1080/10407790.2019.1607117.
29. Li JL, Tang HW, Yang YT. Numerical simulation and thermal performance optimization of turbulent flow in a channel with multi V-shaped baffles. Int Commun Heat Mass Transf. 2018;92(9):39–50. doi:10.1016/j.icheatmasstransfer.2018.02.004.
30. Shi Q, Song C, Pan W, Lei Y. Flow and heat transfer characteristics and comprehensive evaluation of asymmetric plate heat exchangers for centralized heat supply. Appl Therm Eng. 2024;257(1):124306. doi:10.1016/j.applthermaleng.2024.124306.
31. Arsenyeva O, Piper M, Zibart A, Olenberg A, Kenig EY. Investigation of heat transfer and hydraulic resistance in small-scale pillow-plate heat exchangers. Energy. 2019;181:1213–24. doi:10.1016/j.energy.2019.05.099.
32. Roueintan H, Fattahi A. On the pillow-plate heat exchanger with wavy walls and filled with a hybrid nanofluid: numerical simulation and data-assisted prediction. Case Stud Therm Eng. 2024;64(4):105495. doi:10.1016/j.csite.2024.105495.
33. Kanaris AG, Mouza AA, Paras SV. Optimal design of a plate heat exchanger with undulated surfaces. Int J Therm Sci. 2009;48(6):1184–95. doi:10.1016/j.ijthermalsci.2008.11.001.
34. Arsenyeva O, Jaromír Klemeš J, Plankovskyy S, Kapustenko P. The influence of plate corrugation geometry on heat and mass transfer performance of plate heat exchangers for condensation of steam in the presence of air. Therm Sci Eng Prog. 2022;30(10):101248. doi:10.1016/j.tsep.2022.101248.
35. García-Castillo JL, Crespo-Quintanilla JA, Picón-Núñez M. A novel design approach of plate heat exchangers considering the economic impact of chevron angles. Chem Eng Process Process Intensif. 2024;199(6):109759. doi:10.1016/j.cep.2024.109759.
36. Khan TS, Khan MS, Chyu MC, Ayub ZH. Experimental investigation of single phase convective heat transfer coefficient in a corrugated plate heat exchanger for multiple plate configurations. Appl Therm Eng. 2010;30(8–9):1058–65. doi:10.1016/j.applthermaleng.2010.01.021.
37. Krishna M, Swamy M, Manjunath G, Rao N, Rao B, Murthy P. Heat transfer enhancement in corrugated plate heat exchanger. Br J Appl Sci Technol. 2016;18(3):1–14. doi:10.9734/bjast/2016/28438.
38. Hessami MA. An experimental investigation of the performance of cross-corrugated plate heat exchangers. J Enh Heat Transf. 2003;10(4):379–94. doi:10.1615/jenhheattransf.v10.i4.30.
39. Lee J, Lee KS. Friction and Colburn factor correlations and shape optimization of chevron-type plate heat exchangers. Appl Therm Eng. 2015;89:62–9. doi:10.1016/j.applthermaleng.2015.05.080.
40. Kim MB, Park CY. An experimental study on single phase convection heat transfer and pressure drop in two brazed plate heat exchangers with different chevron shapes and hydraulic diameters. J Mech Sci Technol. 2017;31(5):2559–71. doi:10.1007/s12206-017-0454-0.
41. Kim M, Baik YJ, Park SR, Ra HS, Lim H. Experimental study on corrugated cross-flow air-cooled plate heat exchangers. Exp Therm Fluid Sci. 2010;34(8):1265–72. doi:10.1016/j.expthermflusci.2010.05.007.
42. Luan ZJ, Zhang GM, Tian MC, Fan MX. Flow resistance and heat transfer characteristics of a new-type plate heat exchanger. J Hydrodyn Ser B. 2008;20(4):524–9. doi:10.1016/S1001-6058(08)60089-X.